Original Article

Development of a textile sheet mask design for facial care based on a 3D face model of an average woman

Andreja Rudolf[1] iD **, Sonja Šterman[1] and Andrej Cupar[2]**

Abstract

Facial cosmetics moisturise the skin and remove sebum and impurities to maintain healthy skin. Face masks are available on the market in various forms such as gel, emulsion, sheet and paste. The textile sheet mask for facial care is used by all women, regardless of age. This study deals with 3D scanning of women's faces to create an average female 3D face model for the development of a textile sheet mask design for facial care. Screened Poisson surface reconstruction was used to create an average female 3D face model whose dimensions correspond to average dimensions of scanned female faces. A reliable average 3D face model of the women studied was therefore used to develop a textile sheet mask for facial care. A comparison of average facial measurements with the measurements of randomly selected masks on the market revealed differences. Therefore, a design for a textile sheet mask was developed based on average facial measurements and the average 3D face model of a woman and by using virtual prototyping. The use of software for prototyping and simulating the appearance of clothing has also proven to be effective in the development of a textile product such as a textile face mask. The developed pattern design of the textile sheet mask with optimal dimensions and shape adapts to the contours of an average woman's face. This fulfils all the requirements for wearing comfort of the textile sheet mask around the eyes, nose and lips during facial care and enables efficient transfer of the serum from the textile sheet mask to the skin.

Keywords

3D scanning, average woman 3D face model, design of a textile sheet mask, virtual prototyping

Introduction

The skin, as the largest organ, serves as a barrier for microbes to enter the body. Therefore, skin health is an important aspect of personal health and aesthetics. Cosmetic products for the skin are formulated according to skin type, which can change throughout life due to differences in sebum secretion. Cosmetics moisturise the skin and removes sebum and impurities to promote healthy skin.[1–7] Face masks are affordable goods that are easy to apply and have an immediate effect on the skin. They are available on the market in various forms such as gel, emulsion, sheet and paste.[2,5]

The textile sheet masks have been on the market for some time and are very popular within women. They help to remove excess oil and improve the appearance of the skin.

[1]Faculty of Mechanical Engineering, Institute of Engineering Materials and Design, University of Maribor, Maribor, Slovenia
[2]Faculty of Mechanical Engineering, Mechanical Engineering Research Institute, University of Maribor, Maribor, Slovenia

Corresponding author:
Andreja Rudolf, Faculty of Mechanical Engineering, Institute of Engineering Materials and Design, University of Maribor, Smetanova 17, Maribor 2000, Slovenia.
Email: andreja.rudolf@um.si

They are known to moisturise, prevent acne and hydrate the skin. The different types of sheet masks can be categorised by the different types of textiles: cellulose masks with a finer texture, hydrogel masks, bio-cellulose masks, foil masks, knitted cotton masks, ampoule sheet masks and bubble masks.[2,8,9] The popularity of face textile sheet masks is increasing as people become more concerned with improving their facial health-care and beauty. According to research,[10] the use of face sheet masks is expected to increase to USD 701.86 million by 2030.

A facial skin care with a textile sheet mask on which a skin care serum is applied should be comfortable and, in this respect, allow breathing through the nose or mouth while wearing the mask and prevent eye irritation from the serum. At the same time, it must be easy to apply on the face and conform to the contours of the face so that the serum can be efficiently transferred from the mask to the skin. To meet these beautification demands, the pattern design of the textile sheet mask is important, with openings for the eyes, nose and lips and functional slits that can be easily adjusted to the face. Different manufacturers offer different designs of sheet masks adapted to the different anthropometric data of the face. In the study by Liu et al.,[5] comfort, perfect fit, price, sheet mask shape, function and ingredients were identified as the most important factors of sheet mask products whose shape and pattern design were redesigned to better fit the face of an average woman in Taiwan. An international anthropometric study of the facial morphology of different ethnic groups (Europe, Asia, Africa) revealed differences between their anthropometric facial measurements.[11] Fourteen anthropometric measures were studied, measured manually on a sample of 30 men and 30 women in each participating nation. Comparison of these anthropometric measures with those of North American Caucasians showed the least difference with the Caucasian groups in Europe. A study by Choe et al.[12] comparing facial proportions between Korean American and North American groups of 72 women found significant differences in 24 of 26 facial measures. Based on these findings, it can be predicted that women of different population groups need different shapes (pattern designs) and sizes of textile sheet masks for facial care.

Anthropometric measurements can be measured by contact or non-contact methods. Various physical phenomena are used for geometry scanning, such as optical, laser, dark field, ultrasonic, roentgen radiation or variations of composite scanning. The scanning process can also vary in terms of speed, accuracy and health compatibility. 3D scanning processes that are harmless to health are suitable for 3D scanning of the human body. Optical and laser 3D body scanning technologies have been researched with the aim of obtaining accurate 3D body models.[13–21] These enable the determination of reliable 3D body measurements required for the creation of sizing systems for clothing and/or the development of garment pattern designs.

The construction of average 3D human body models or 3D models of body parts of a given population is extremely important for the development and testing of products in various fields. Any generalisation of a 3D model requires a base of 3D models, that is, scans or 3D meshes, which are properly processed using various software and processing techniques to successfully fuse them into a general 3D model. Some generalised 3D models are based on anthropometric data, such as a virtual 3D model of the human hand for ergonomic product design.[22,23] Others create generalised 3D human body models as 3D average meshes based on 3D scanned people especially for computer animation, biomedical analysis, and human-centred product development, as well as garment pattern designs development using virtual prototyping of garments on generalised parametric 3D human body models in the clothing industry.[24–30] Average 3D face models were created for two European groups (Slovenia and Wales) using 3D data acquired with a laser scanning system and a previously validated mathematical algorithm.[31] They deployed an average 3D face model versus scan comparison using software GOM Atos with the following protocol: 3D mesh editing and alignment, reconstruction of the average 3D mesh and creation of the average 3D face model. For case of orthodontic 3D digital model of mandibula surface-to-surface matching method for scanned 3D meshes alignment was used, that is, the best-fit method with the least-mean-squared algorithm.[32]

Human body scanning was established as 3D human body acquisition and measurement tool also for garment prototyping.[33,34] These measurements could serve as anthropometric data from which an average 3D model can be created, as in the study by Božič et al.[31] To extract the average mesh on top of all 3D meshes, Poisson surface reconstruction or improved derivates of Poisson surface reconstruction were deployed.[35–37] Screened Poisson surface reconstruction is improved version of 3D mesh reconstruction on top of 3D point cloud or 3D meshes. It produces one smooth, continuous 3D mesh and is included in many 3D software, also in MeshLab and HP 3D Scan.[38,39]

The face sheet mask for skin care is used by all women, regardless of age. Therefore, the product is adapted to the anthropometric characteristics of a specific female population, that is, to average face dimensions. As the facial morphology of different ethnic groups differs, there is a need for different shapes (pattern designs) and sizes of textile sheet masks for facial care that allow the mask to be applied correctly. It must fit the contours of the face to effectively transfer the serum to the skin and must not obstruct the user's viewing or breathing. Particular attention must therefore be paid to the size and position of the openings for the eyes, nose and lips. In this study, average face dimensions are examined using 3D scans of the female group from Slovenia with the aim to compare them with measurements of different textile sheet masks
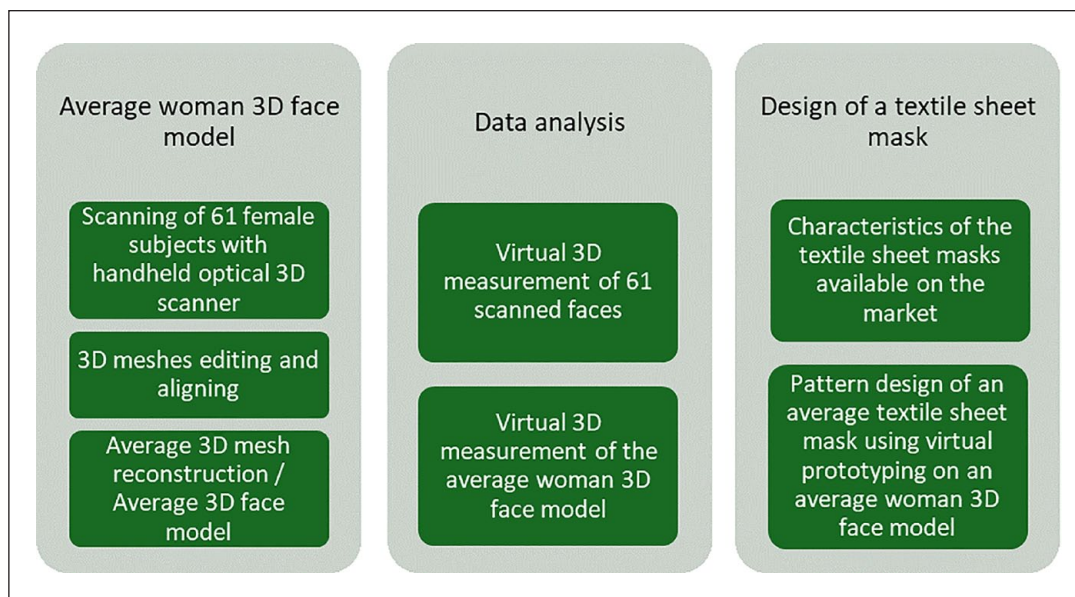
Figure 1. Research model.

on the market and to develop a textile sheet mask design with optimal measurements and shape for the female population studied. Based on scans, Screened Poisson surface reconstruction was used to create an average woman 3D face model, dimensions of which were compared with average dimensions of the face of female population studied and used to develop a design of textile face sheet mask.

Methods

Figure 1 shows the research model for the development of a 3D face model of an average woman using a 3D face scan and the development of a design for a textile sheet mask.

Average woman's 3D face model

The simplified flowchart in Figure 2 shows the steps required to create an average 3D face model. The 3D scan is created with a 3D scanner. These 3D point clouds are polygonised into the 3D mesh, one for each scanned face. This polygonization already reconstructs the mesh using Poisson surface reconstruction[40] in the Sense 3D software. In the next step, all 3D face meshes are imported into one file in which the meshes must be edited and aligned, as explained in detail in Section 2.1.2. The next step is an octree that manages 3D data in a data structure where observed spatial elements become denser, which is achieved by subdividing in the areas where details appear on a 3D model.[41] Furthermore, Screened Poisson surface reconstruction is performed, where the final solution is the average 3D mesh face model.

3D face scanning. The study involved a group of 61 female subjects from Slovenia whose ages ranged from 20 to 58 years and who had different body heights (BH), body weights (BW) and body mass indexes (BMI). The basic average data of measured female participants are shown in Table 1.

The Sense 3D scanner with combined technology of laser class 1 and structured light was used. Laser class 1 poses no danger to human eyes or skin.[42] The scanner has a spatial x/y resolution at 0.5 m of 0.9 mm and a depth resolution at 0.5 mm of 1.0 mm.[40] Sense 3D second generation is a handheld scanner from 3D Systems with Intel camera sensor and automatic object recognition for scan alignment. The scanning area was limited to a body part.

In 61 female participants study, the head was scanned from the front and from the left and right sides, that is, the area of the face from the crown to the ears, over cheeks and chin to the neck, Figure 3. Prior to scanning, a tight-fitting cap was placed on the participant's head so that it accurately covered the scalp, and a pyramid-shaped marker was placed on the top of the head. A clear line of the face, required for facial treatment with a textile sheet mask to the top of the head, was captured for further measurement of the face and head height.

3D meshes editing and aligning. Every scanning software handles 3D data differently, but a 3D point cloud is created after every 3D scan. This 3D point cloud serves as the basis for the 3D mesh of the object. 3D scans were created using the 3D scanner Sense,[40] then automatically polygonised using the Poisson surface reconstruction and exported as an STL file by the Sense software without additional editing. Gom Inspect software proves to be a
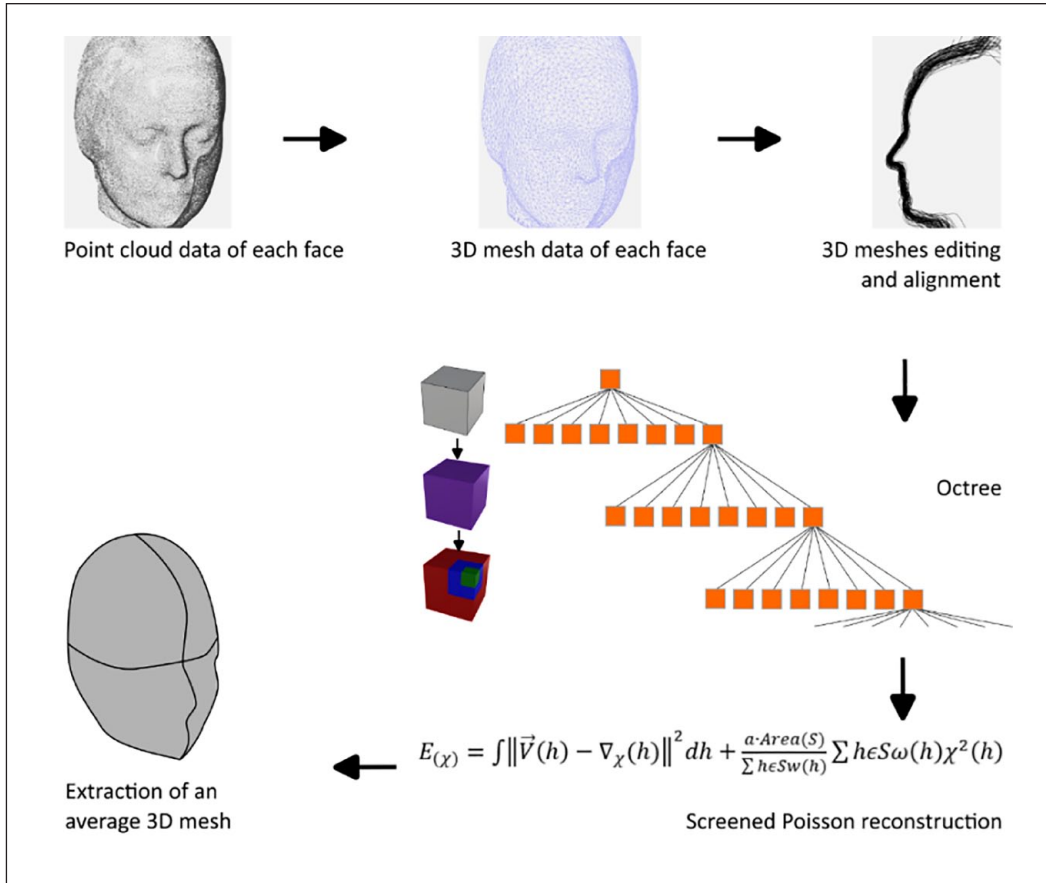
Figure 2. Simplified flowchart for the creation of a 3D face model of an average woman.

Table 1. Basic data of the measured participants.

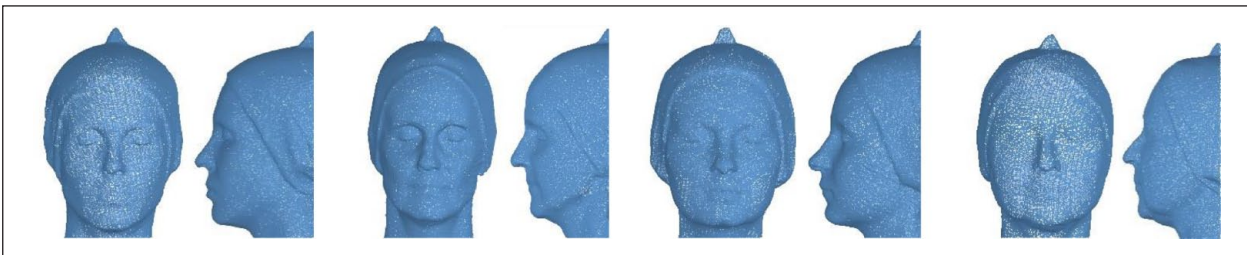| Age and body attributes	Symbol	$\bar{x}$ (x_{min}; x_{max})	SD (cm)	CV (%)
Age (years)	A	35.98 (20; 58)	11.82	32.86
Body height (cm)	BH	166.38 (154.00; 180.00)	5.81	3.49
Body weight (kg)	BW	65.20 (45.00; 101.00)	13.07	20.05
Body mass index	BMI	23.54 (16.90; 35.43)	4.51	19.15

Figure 3. Examples of 3D facial scans frontal and lateral in the software sense.

more suitable tool for mesh editing such as cleaning, mesh unification, mesh decimation and smoothing.[43] Alignment or registration is a process of adjusting the position and rotation of 3D scanned female face meshes to the correct position in 3D space. It was also performed in Gom Inspect according to the Multilevel active registration described in detail in Rudolf et al.[21] and Kozar et al.[44] In the following, the process of aligning 3D scans was necessary to create
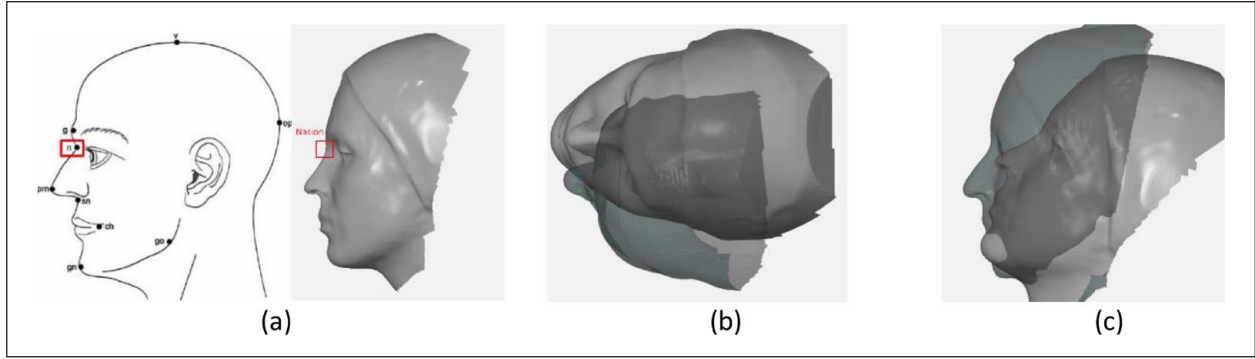
Figure 4. Aligning of scans in the nasion (a), left-right symmetry (b) and rotation (c).

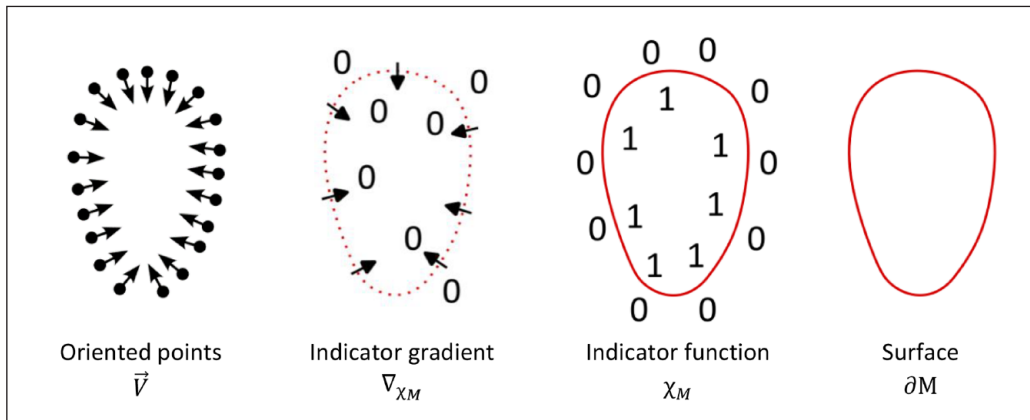| Oriented points $\vec{V}$ | Indicator gradient ∇_{χ_M} | Indicator function χ_M | Surface ∂M |

Figure 5. Simplified Poisson surface reconstruction process using a 2D example.

an average 3D mesh face model, which is summarised as follows: (a) all scans were aligned using the manual method to obtain a well-presented averaged 3D mesh, that is, observation and alignment of scans in the nasion (intersection of the frontonasal and intranasal sutures[45]), (b) adjustment of left-right symmetry and (c) rotation of each scan, as shown in Figure 4.

Average 3D mesh reconstruction. An average mesh of the 3D face model was created from 61 3D meshes registered on top of each other. For the reconstruction of an average 3D mesh, also called fusion, the screened Poisson surface reconstruction was used. Software involved in the 3D mesh reconstruction process was HP 3D scan 5.6.0 that supports 3D scanner HP SLS and uses Screened Poisson surface reconstruction for scans fusion.[39] All 61 scans were separately imported in HP 3D scan software.

Poisson surface reconstruction is an implicit method often used for the reconstruction of 3D scan data of static objects. It robustly approximates noisy data with very smooth surfaces. The Poisson surface reconstruction method is based on vector fields ($\vec{V}$). With indicator gradient (∇_{χ_M}) defines indicator function (χ_M) and finally reconstructs a model with watertight closure features,

geometric surface properties and detail features (∂M). For a better understanding, the reconstruction process is simplified using the 2D example in Figure 5, while it works in the same way in the additional third dimension. Detailed explanations and practical examples for the Poisson surfaces reconstruction and Screened Poisson surface reconstruction can be found in Kazhdan et al.,[35] Kazhdan and Hoppe[36] and Liu et al.[37] In Screened Poisson surface reconstruction, position and normal constraints are considered simultaneously, which means that the mesh is denser where details are present. This reduces the compute calculation time and improves the results of the 3D mesh.[36]

In the vector field $\vec{V}$ we are looking for the solution to the function $\tilde{\chi}$, whose gradient $\tilde{\chi}$ is closest to $\vec{V}$, which is the solution of the Poisson equation $\Delta\tilde{\chi} = \nabla \cdot \vec{V}$.

The original Poisson surface reconstruction algorithm adjusts the implicit function by applying a single global offset to ensure that its average value is zero at all points. However, the presence of errors can cause the implicit function to drift, making it impossible to find a satisfactory global offset. To solve this problem, an alternative approach was proposed in Kazhdan and Hoppe,[36] where the points are explicitly interpolated. Therefore, the

equation for the screened Poisson surface reconstruction $(\Delta - \alpha \tilde{I})\chi = \nabla \cdot \vec{V}$ is presented. $\mathcal{P}$ is points set with the weights $w: \mathcal{P} \to \mathbb{R}^{\geq 0}$, and the energy denoted by E in equation (1). To balance the two energy terms in equation (2), the screening parameter α should be adjusted so that the reconstructed 3D surface is scaling irrelevant and the extension of a solution at a coarse depth is an accurate estimate at a finer depth solution. Both goals can be achieved by adjusting the weighting of the position and gradient constraints at different octree depths. The magnitude of the gradient constraint scales with the resolution, so the weight of the interpolation constraint must be doubled with each depth[36,37]:

$$E_{\vec{V}}(\chi) = \int \left\| \vec{V}(p) - \nabla_\chi(p) \right\|^2 dp \qquad (1)$$

$$E_{(w,\mathcal{P})}(\chi) = \frac{\alpha . Area(S)}{\sum_{h\epsilon} Sw(h)} \sum_{h\epsilon} S\omega(h)\chi^2(h) \qquad (2)$$

where h is the sample point, ∇_χ is the gradient of the indicator function, $Area(S)$ is the reconstructed surface region, α is the screening factor, used to measure the fitting gradient and fitting value and $\omega(h)$ is the sample point weight.[37]

Virtual 3D measuring of scanned face dimensions

Measurements of face dimensions were taken to determine average face dimensions with the aim of evaluating an average 3D face model and designing an average textile sheet mask for face care. Examined were head length and those face dimensions that have impact on the development of a textile sheet mask pattern design. Some of the dimensions that correspond to anthropometric points for a precise study of facial morphology are explained in detail in Farkas et al.,[11] Uzomba et al.[46] and Leth-Steensen[47] while the rest are important for the construction of the textile sheet mask pattern design. The 12 dimensions of the face were measured: scalp–nose length (trichion–nasion length, i.e. forehead height), nose length (nasion–subnasale length), nose–lip lower edge length (subnasale–cutaneous lower lip), lip lower edge–chin length (dimension from the cutaneous lip lower edge to the most anterior–inferior point of the chin contour, i.e. gnathion), eye socket height (eye socket, also called orbit, which is the part of the skull surrounded by the forehead, temple, cheeks and nose), lip height (height from cutaneous upper to lower lip), face width at the eyes level, nasal bridge width, eye socket width, nose width (alare–alare, i.e. morphological nose width), lip width and chin width, Figure 6.

The virtual 3D measurement of 61 scanned faces and the average 3D face model were performed using OptiTex 3D software and the tool Add Tape Measure. The face measurements were repeated three times consecutively.
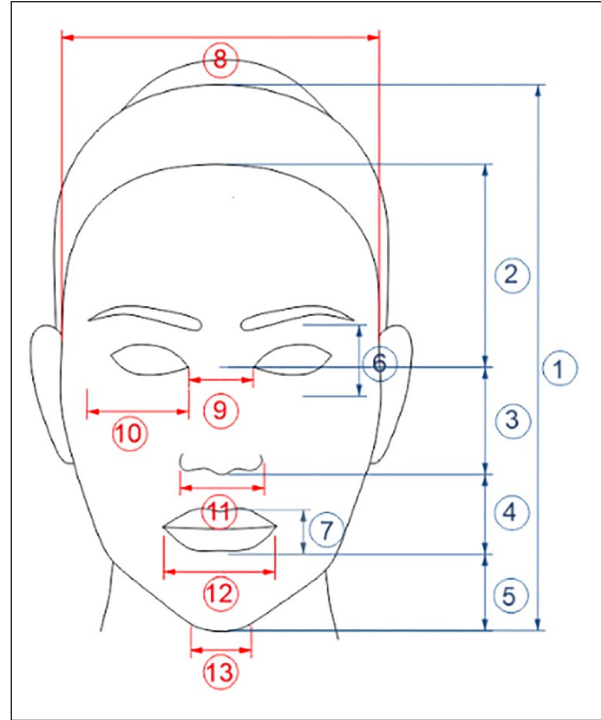

Figure 6. Measurement of face dimensions: (1) head length, (2) scalp-nose length, (3) nose length, (4) nose-lip lower edge length, (5) lip lower edge-chin length, (6) eye socket height, (7) lip height, (8) face width at the eyes level, (9) nasal bridge width, (10) eye socket width, (11) nose width, (12) lip width and (13) chin width.

Data analysis

The mean values ($\tilde{x}$), Standard Deviations (SD) and Coefficients of Variation (CV) were calculated for measurements of faces dimensions. Differences (D) were calculated between averaged measurements of Scanned Faces (SFs) and average measurements of 3D Face Model (3DFM). A positive value (+) means that the SFs is greater than the 3DFM and a negative value (−) vice versa.

Design of a textile sheet mask for face skin care

An analysis of six textile sheet masks for facial treatment from different, randomly selected manufacturers was carried out to compare their dimensions and shapes with a newly designed textile sheet mask for a studied group of women. The surface mass and thickness of dry sheet masks were measured to determine basic properties of textile substrate. Wet textile sheet masks were placed between two sheets of soft paper to absorb excess moisture, placed on a dry sheet of paper, dried and conditioned under standard conditions, prior to measurements. Depending on the design of the mask (shape and size), the thickness of the textile could be measured at four different points according to the ISO 5084:1996 standard,[48] while three
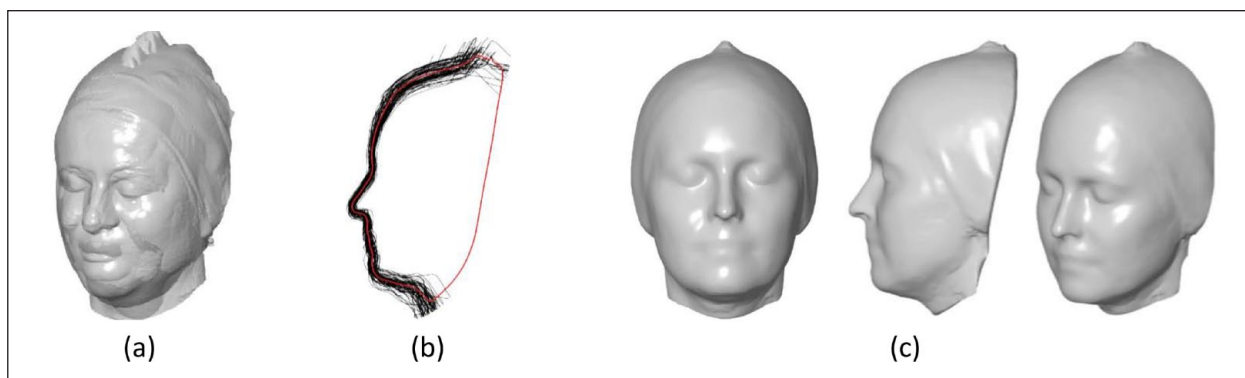
Figure 7. Creation of an average woman 3D face model, (a) Scans aligned on top of each other, (b) 2D longitudinal sections of meshes and the average mesh (red), and (c) Average woman 3D face model.

50×50 mm squares were cut from each textile mask to determine the weight. The weight is calculated and expressed in g/m^2 as in the standard ISO 3801:1977.[49] At the same time, specific characteristics were given for each mask, such as the purpose of care and the duration of the facial treatment, the textile material and other characteristics of the mask shape.

The construction of the textile sheet mask 2D pattern design for an average women's face care was based on the SFs and 3DFM dimensions with help of the OptiTex PDS system. The purpose of development of the sheet mask 2D pattern design is to provide the studied group of women a sheet mask that fit them well for effective facial care and allows them to rest comfortably during application. Designed textile sheet mask for facial treatment was tested on the average 3D face model.

Results with discussion

The average 3D face model

The 3D scans were imported separately into the HP 3D scan software to perform the fusion process with the Screened Poisson surface reconstruction.[39] They were aligned on top of each other using the Gom Inspect software and the Multilevel active registration tool, as shown in Figure 7(a). Based on 61 scans, a reconstructed, 3D average mesh was created. Figure 7(b) shows 2D longitudinal sections of all meshes side views of the 3D scans. The red curve represents the average longitudinal section of the mesh that visually appears in the centre of all sections, which also confirms the average model.

Reconstructed 3D mesh of an average woman 3D face model was exported from HP 3D scan software and imported into existing project in software Gom Inspect to close, regularise, and smooth 3D face model with Gom Inspect's tools for final mesh editing. The final average woman 3D face model has a uniform surface, with no irregularities, which proves that enough subjects were included in the study, Figure 7(c).

Comparison of dimensions of an average real face and a 3D model of the average face

The mean values ($\bar{x}$), Standard Deviations (SD) and Coefficients of Variation (CV) for both real scanned faces (SFs) and an average 3D face model (3DFM) of female are presented in Table 2. In addition, the minimum and maximum values of each body dimension, calculated differences (D) between the mean values of the SFs and 3DFM are given in Table 2.

The research shows that the group of women studied has different faces. They differ least in the dimensions of head length, head width at eye level, nose length, eye socket width, scalp-nose length, nose width, nose-lip lower edge length, lip width and eye socket height (SFs: CV between 4.50% and 9.99%). Larger differences are observed between dimensions of nasal bridge width, lip lower edge-chin length and lip height (SFs: CV between 10.37% and 11.52%). Largest differences are observed in the chin width dimension, which was difficult to measure using a non-contact method due to the diversity of facial morphologies and the indistinct chin width of some faces (SFs: CV 20.94%). Differences in facial morphology of female and male Slovenian population are also confirmed in the study by Božič et al.[31]

The average 3D face model (3DFM) of the woman shows a significantly small deviation from the average dimensions of scanned faces (SFs). The differences range from 0.41 mm (−0.89%) for the chin width and 1.15 mm (1.63%) for the scalp-nose length. Based on extensive measurements of the SFs and measurements of a 3DFM, it can be confirmed that a reliable average 3D face model of the women studied was created by using a Screened Poisson surface reconstruction. It can therefore be used for the development of a textile sheet mask for facial care.

Table 2. Measurements of the average real face and 3D model of an average face.

Face dimensions	Averaged measurements of scanned faces (SFs)			Average measurements of 3D face model (3DFM)			Difference	
	$\overline{SFs}$ (mm) SFs_{min} (mm) SFs_{max} (mm)	SD (mm)	CV (%)	$\overline{3DFM}$ (mm) $3DFM_{min}$ (mm) $3DFM_{max}$ (mm)	SD (mm)	CV (%)	$D_{\overline{SFs-3DFM}}$ (mm)	$D_{\overline{SFs-3DFM}}$ (%)
Head length	225.58 198.96 246.06	10.14	4.50	224.36 219.99 225.79	1.70	0.76	1.22	0.54
Scalp-nose length	71.74 58.05 83.54	5.74	8.00	70.59 69.23 72.85	1.19	1.69	1.15	1.63
Nose length	45.79 35.94 53.23	2.84	6.20	45.25 44.28 46.15	0.63	1.40	0.54	1.19
Nose-lip lower edge length	38.51 32.47 48.86	3.56	9.24	38.76 37.51 39.95	0.77	1.97	−0.14	−0.35
Lip lower edge-chin length	27.06 22.07 35.50	2.97	10.96	27.13 25.75 28.84	1.07	3.95	−0.07	−0.26
Eye socket height	36.47 28.06 46.32	3.64	9.99	36.24 35.03 37.70	0.87	2.40	0.23	0.64
Lip height	25.62 20.16 34.00	2.95	11.52	25.36 23.72 27.07	1.06	4.18	0.27	1.05
Head width at the eyes level	132.68 117.85 153.88	6.79	5.12	132.58 130.10 135.92	1.93	1.46	0.10	0.07
Nasal bridge width	21.72 16.24 26.04	2.25	10.37	21.74 20.77 23.49	0.91	4.17	−0.01	−0.07
Nose width	33.17 24.07 37.16	2.67	8.05	33.30 32.50 34.63	0.75	2.26	−0.13	−0.38
Eye socket width	45.66 34.91 54.39	3.49	7.64	45.81 44.70 47.45	0.94	2.06	−0.15	−0.34
Lip width	53.53 42.32 64.48	5.00	9.35	52.77 51.67 54.12	0.85	1.60	0.76	1.44
Chin width	45.61 29.56 82.25	9.55	20.94	46.02 44.58 47.45	0.91	1.98	−0.41	−0.89

Development of the design of a textile sheet mask for facial care

Six face sheet masks from different manufacturers, randomly selected, were subjected to analysis of (a) dimensions of selected textile sheet masks: maximum mask width, maximum mask length, scalp-nose length, nose length, nose-lip opening length, lip opening height, lip-chin length, eye opening width and height, distance between eye openings, nose opening width, lip opening width and height, (b) shapes and (c) essential characteristics, Tables 3 and 4.

The measured maximum width of textile sheet masks ranges from 210 to 247 mm and the maximum length from

Table 3. Dimensions of the researched textile sheet masks.

Dimensions (mm)	Sheet mask 1	Sheet mask 2	Sheet mask 3	Sheet mask 4	Sheet mask 5	Sheet mask 6	New sheet mask
Mask width (max)	247	234	210	225	245	225	190
Mask length (max)	210	200	199	210	205	200	184
Scalp-nose length	82	70	80	80	80	80	72
Nose length	46	44	54	49	42	48	46
Nose-lip opening length	14	16	13	18	28	12	26
Lip opening-chin length	50	50	30	44	52	43	27
Eye opening width	50	55	55	50	40	50	46
Eye opening height	25	20	25	28	20	20	36
Distance between eye openings	28	29	22	24	35	25	22
Nose opening width	45	53	64	50	47	48	65
Lip opening width	58	63	65	60	55	63	54
Lip opening height	18	20	22	19	13	17	26

Note. The shaded cells indicate the dimensions of the sheet masks that best match the dimensions of the 3DFM and the new sheet mask (shaded last column).

Table 4. Basic properties of the analysed face mask designs and a new sheet mask design.

	Sheet mask 1	Sheet mask 2	Sheet mask 3	Sheet mask 4	Sheet mask 5	Sheet mask 6	New sheet mask
Shapes							

Characteristics							
Use	Moisture and rich care	Restores elasticity	Hydrating	Elasticity, reshape	Moisture, smooth, refresh	Restore, moisture	Under research
Apply	15–20 min	20 min	30 min	10 min refrigerator, 10 min treatment	15 min	15 min	Under research
Textile material	Nonwoven	Nonwoven	Hydrogel with cornflower extract	Nonwoven (paper techn.)	Nonwoven	Nonwoven (biodegradable)	Under research
Weight (g/m^2)	62.56	51.52	/	47.60	67.97	41.08	
SD (g/m^2)	3.94	5.97		3.50	1.39	1.57	
CV (%)	6.30	11.64		7.35	2.04	3.83	
Thickness (mm)	0.28	0.34	/	0.34	0.34	0.40	
SD (mm)	0.01	0.01		0.01	0.01	0.01	
CV (%)	4.71	2.87		3.16	3.39	3.35	
Other	Slits – eye, nose, chin	Slits – eye, nose, chin	Mask in two parts; slits – nose, chin	/	Chin slits	Slits – eye, nose, chin	Slits – eyes, nose, chin

199 to 210 mm, Table 3. The length of the scalp-nose is quite similar and is 80 mm for four masks and 70 and 82 mm for remaining two masks. They differ from each other in all other measured dimensions. The nose length varies for all masks and is between 42 and 54 cm. The length of the nose-lip opening has a wide range between sheet masks, between 12 and 28 mm, as does the length of the lip opening-chin between 30 and 52 mm. The eye opening width of 50 mm is the same in three masks, two are 55 mm and one is 40 mm. Also, three masks have the same eye opening height of 20 mm, two of 25 mm and one of 28 mm. The distance between eye openings is between 22 and 35 mm. The width of the nose opening varies in all masks and is between 45 and 64 mm. The width of the lip opening (55–65 mm) and the height of the lip opening (13–22 mm) also vary.
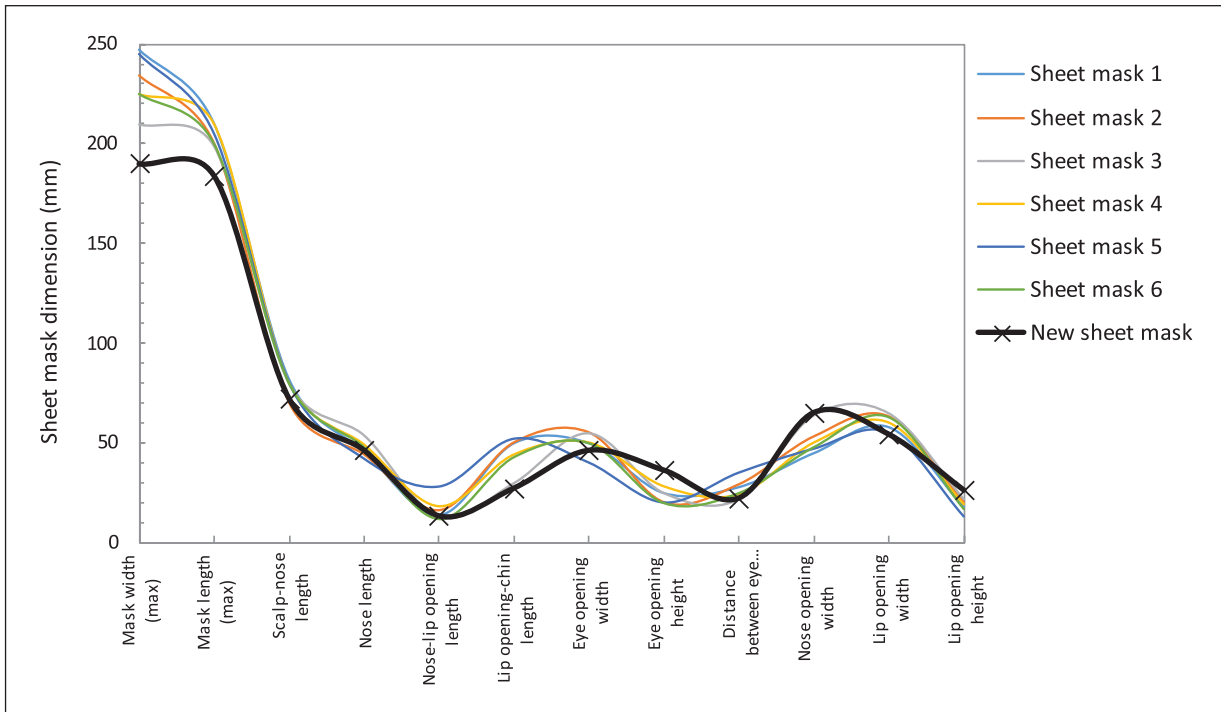
Figure 8. Comparison of the dimensions of textile face sheet masks.

Dimensions for a new design of a textile sheet mask can be found in the last column in Table 3, which contains the already measured 3DFM dimensions (Table 2) and additional dimensions required for the development of the pattern design of the textile sheet mask, which were measured on the 3DFM. In Table 3, the dimensions of sheet masks that best match the dimensions of the 3DFM are shaded. However, a comparison of the dimensions of textile sheet masks clearly shows that no mask completely matches the dimensions of the 3DFM, Figure 8, as well as the dimensions of the face sheet mask proposed in the study of Liu et al.[5]

The biggest difference in dimensions is in the height of the eye opening, whose maximum dimension is 28 mm, while this dimension is 36.5 mm for the SFs and 36.2 mm for the 3DFM. It is assumed that the difference is related to the measured distance of the eye height. In this study, the height of the eye socket was measured to ensure unobstructed view when using a mask and to prevent possible transfer of the serum to the eyes. The width of the sheet mask was adjusted to the width of the face from scalp to scalp at the eye line. For this purpose, the length from the eye socket to the scalp (38 mm) was measured on the 3DFM. The required width of the nose opening was measured at the 3DFM (length from one nostril to the other across the tip of the nose), which is 65 mm. The four analysed masks have a nose opening width between 45 and 53 mm, while in mask 3 this is 64 mm, which is almost the same measurement as ours. The width of the lip opening is

between 55 and 65 mm in the sheet masks analysed, whereby this dimension corresponds most closely to our measurement in the fifth sheet mask. The height of the lip opening is between 13 and 22 mm. The third sheet mask corresponds most closely to our mask, which has a lip opening height of 26 mm, which is higher than all the masks analysed. The latter is due to the measurement of the height of the lip opening from the cutaneous upper lip to the lower lip, on the assumption that a higher lip opening provides better comfort during care with a textile sheet mask and prevents possible transfer of the serum into the mouth.

By analysing the comparison between the randomly selected masks and the measurements of the average woman's face studied, it can be concluded that the third mask, which has similar six measurements, could fit our average woman face best. However, there are significant differences in the measurements of the scalp-nose length, the nose length, the width and length of the eye opening and the width of the lip opening. The latter was taken into account in the development of the new textile sheet mask to ensure unhindered viewing and breathing and to avoid the discomfort caused by the possible transfer of serum into the eyes and mouth due to the small openings.

The basic characteristics of analysed face sheet masks designs are shown in Table 4. It can be observed that masks have different shapes. All have a slit in the nose area, but in different shapes and lengths. Four of six masks also have slits in the chin and eye area to better fit the face (1,
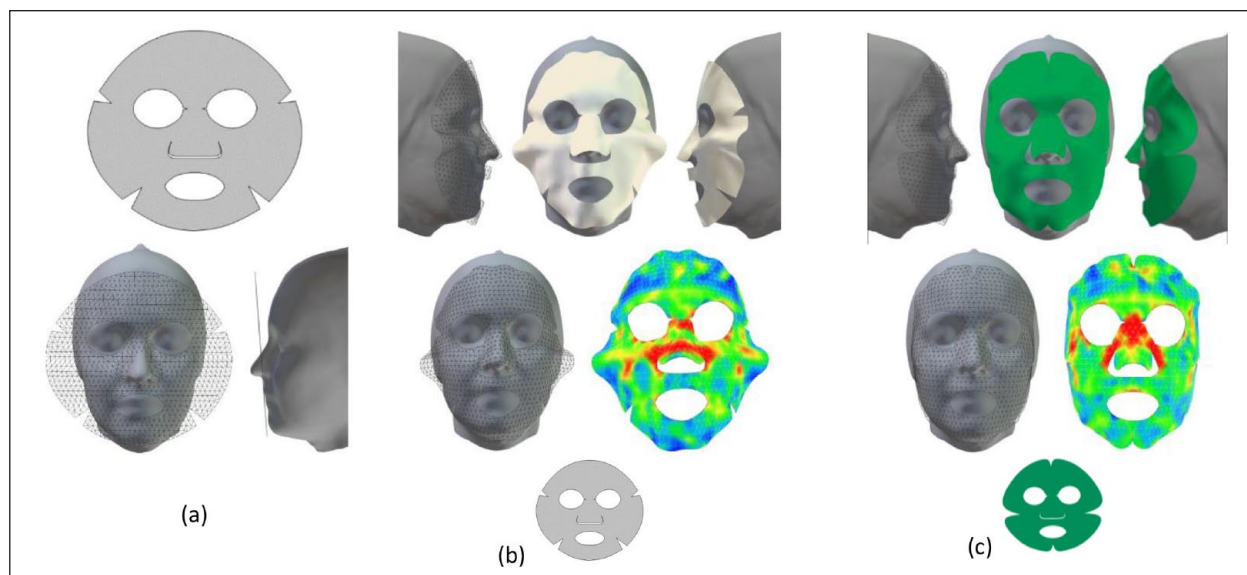
Figure 9. Development of the new textile sheet mask design, (a) First pattern design positioned on the 3DFM, (b) First virtual prototype, and (c) New design of the textile sheet mask.

2, 5, 6). The sheet mask 3 consists of two parts – the upper part covers the face up to the end of the nose, while the lower part covers the facial area from the nose to the chin. The sheet mask 5 has no slits in the chin and eye area. Sheet masks analysed are intended for moisturising and rich care, restoring elasticity, smoothing and refreshing the skin and contain various serums with coconut milk, hyaluronic, collagen, probiotic fractions, etc., whose recommended duration of care varies (10–20 min).

The textile substrate of analysed face sheet masks is a non-woven textile (1, 2, 4–6), while the third face sheet mask uses hydrogel with cornflower extract as the substrate for the application of the serum for face care, Table 4. They also vary in weight and thickness. Their weight ranges from $41.08 \, \text{g/m}^2$ (6) to $67.87 \, \text{g/m}^2$ (5) and their thickness from 0.28 mm (1) to 0.40 mm (5). The thickness and weight of a sheet mask 3 could not be measured correctly, as a dry mask becomes thinner and more wrinkled. This data is therefore not included.

The pattern design of a face sheet mask was constructed based on the average facial measurements of the group of women studied, rounded to the nearest millimetre, Table 3, and additional measurements were taken on the 3DFM as previously described. The first pattern design of the textile sheet mask has slits in the areas that can also be seen in textile sheet masks examined, allowing the sheet mask to fit better on the nose, Figure 9(a). The nose slit consists of 16 mm long diagonal lines and a 4 mm long nose slit on the inner edge of the eye openings. The slits are also located in the chin area and on the side of the forehead near the eyes in the form of cut-out darts, so that the sheet mask can be fitted to the face with less wrinkling of the textile material, which is necessary to better transfer the serum from the mask to the face.

To simulate the fit of the textile sheet mask on the 3DFM, it was rotated 90 degrees from its natural vertical position to a horizontal position that the sheet mask can be draped on the 3DFM. The face sheet masks made of real textile are very flexible when soaked with serum. Therefore, the mechanical properties of a single knit jersey (88% polyester, 12% spandex) from the OptiTex 3D Fabric Library with an average weight of analysed textile sheet masks ($54.0 \, \text{g/m}^2$) and thickness (0.34 mm) were used for the simulation to obtain a flexible textile structure similar to a textile sheet mask with a serum. The simulation parameters were set to default values and the mesh density of the 3D textile model was 0.5 cm, Figure 9(a).

The first virtual prototype of the textile sheet mask shows correctly dimensioned and positioned openings for the eye sockets, nose and lips, Figure 9(b). There is a slight sagging of the textile under the nose and through the lip opening, which cannot be avoided during simulation and is normal due to the draping properties of the textile, as the mask is not wetted with serum. It can be seen that the prototype of the textile sheet mask fits the 3DFM well in the forehead and chin, while larger folds appear in the cheek area, even though the slits were used in the form of darts in the chin area and on the side of the forehead near the eyes. The maximum tension of the textile (red) is distributed in the area of the nose and continues over the cheekbones (red, orange), which consequently forms a fold on the cheeks, Figure 9(b). This is due to the nose slit being too short and the inadequate position of the slits to fit the mask to the face. The latter refers to the need for slits in the cheek and nose area so that the textile sheet mask can adapt well to the face without forming unnecessary folds, making it easier to place on the face and more comfortable to wear during facial care. Using the virtual prototyping

process and after several iterations of the pattern design of the textile face sheet mask, the design of the textile face sheet mask was adapted in the cheek area and the slits for the nose were enlarged to 26 mm, Table 4. Figure 9(c) shows a simulation of the new design of the textile sheet mask on the 3DFM. It can be seen that the maximum tension of the textile (red) is concentrated in the nose area. This means that longer nose slits allow the mask to fit better to the nose and therefore also to the cheek, which is emphasised by slits in the new position on the sides. A new design of the textile sheet mask also adapts well to the 3DFM in the area of the forehead and chin. A slight sagging of the textile under the nose and through the lip opening can be observed and cannot be avoided in the simulation due to the draping properties of the textile.

It can be assumed that the use of software for prototyping and simulating the appearance of clothing has also proven to be effective in the development of a textile product such as a textile face mask. A new design of the textile face sheet mask allows a good fit of the mask to the analysed average 3D female face model and offers a better wearing comfort than the other analysed masks, especially in the area of the eyes, nose and mouth, which allows unobstructed vision with the eyes and breathing through the nose and mouth, and the eyes are not irritated by the serum. On the other hand, the shape of the mask itself allows for easier application on the face without unnecessary adjustment to the facial contours by folding the mask, which enables perfect transfer of the serum from the mask to the face during care. In future research, the textile sheet mask will be tested on real test subjects with different facial morphologies.

The shape of the textile face sheet mask is reminiscent of a butterfly. In various cultures, butterflies are symbols of transformation, hope and rebirth and evoke the qualities of freedom, beauty and love, which users can also harmonise their facial care with.

The developed design of the textile face sheet mask is part of a project in which future research is aimed at the sustainable development of the textile sheet mask as a complete product. The focus is on analysing and developing the appropriate textile for the face sheet mask, the treatment serum, which will add new dimensions to facial care, and the overall design of the sheet mask packaging.

Conclusions

The aim of this study was to create an average woman 3D face model in order to develop a design for a textile sheet mask with optimal measurements and shape for the women studied. Based on the 3D scans of the 61 women, an average 3D face model (3DFM) of the woman was created using a Screened Poisson surface reconstruction. The comparison between the measurements of the SFs and the

measurements of a 3DFM showed that a reliable average 3D face model of the women studied was created by using a Screened Poisson surface reconstruction. Therefore, it was used for the development of a textile sheet mask for facial care. A comparison of the dimensions of randomly selected textile sheet masks on the market clearly shows that no mask completely matches the dimensions of the 3DFM. The pattern design of a textile face sheet mask was created on the basis of average facial dimensions of the group of women studied and additional measurements of the 3DFM. The design of a textile sheet mask developed with the help of virtual prototyping on 3DFM enables optimal fit to the average face in the area of the forehead, eyes, nose, lips, cheeks and chin. It therefore enables improved comfort during facial care, that is, unhindered viewing and breathing through the nose and mouth, while the eyes and mouth are not irritated by the serum thanks to appropriately designed openings.

Textile sheet masks are used to moisturise and richly nourish the face, restoring elasticity, smoothing and refreshing the skin with various serums containing coconut milk, hyaluronic acid, collagen, probiotic fractions, etc. Future research will therefore focus on the sustainable development of the sheet mask as a complete product. The focus is on analysing and developing the textile for the sheet mask, the serum for the sheet mask, which would add new dimensions to facial care, and the overall design of the textile sheet mask packaging.

ORCID iD

Andreja Rudolf https://orcid.org/0000-0001-8658-0859

References

1. Yu B, Kang SY, Akthakul A, et al. An elastic second skin. *Nat Mater* 2016; 15: 911–918.
2. Nilforoushzadeh MA, Amirkhani MA, Zarrintaj P, et al. Skin care and rejuvenation by cosmeceutical facial mask. *J Cosmet Dermatol* 2018; 17(5): 693–702.
3. Fan L, Jia Y, Cui L, et al. Analysis of sensitive skin barrier function: basic indicators and sebum composition. *Int J Cosmet Sci* 2018; 40: 117–126.

4. Draelos ZK. Cosmetics: an overview. *Curr Probl Dermatol* 1995; 7(2): 45–64.

5. Liu B, Lin S, Lien C, et al. Determined the critical factors of facial mask products and size design. In: *Proceedings of the 2014 IEEE international conference on management of innovation and technology*, Singapore, 23 September 2014.

6. Youn SW, Kim SJ, Hwang IA, et al. Evaluation of facial skin type by sebum secretion: discrepancies between subjective descriptions and sebum secretion. *Skin Res Technol* 2002; 8(3): 168–172.

7. Youn SW. Cosmetic facial skin type. In: Humbert P, Maibach H and Fanian F, et al. (eds) *Measuring the skin*. Cham: Springer, 2015, pp.1–6.

8. BelMondo. Types of sheet mask fabrics, https://belmondobeauty.com/types-of-sheet-mask-fabrics/ (accessed 2 November 2023).

9. The Klog. The 8 different types of sheet masks and when to use them, https://theklog.co/different-types-sheet-masks/ (accessed 2 November 2023).

10. Data Bridge. Global sheet face masks market – industry trends and forecast to 2030, https://www.databridgemarketresearch.com/reports/global-sheet-face-masks-market (2022, accessed 2 November 2023).

11. Farkas LG, Katic MJ and Forrest CR. International anthropometric study of facial morphology in various ethnic groups/races. *J Craniofac Surg* 2005; 16(4): 615–646.

12. Choe KS, Sclafani AP, Litner JA, et al. The Korean American woman's face: anthropometric measurements and quantitative analysis of facial aesthetics. *Arch Facial Plast Surg* 2004; 6(4): 244–252.

13. Gill S. A review of research and innovation in garment sizing, prototyping and fitting. *Text Prog* 2015; 47: 1–85.

14. Bragança S, Arezes P, Carvalho M, et al. Current state of the art and enduring issues in anthropometric data collection. *DYNA* 2016; 83: 22–30.

15. Gill S and Parker CJ. Scan posture definition and hip girth measurement: the impact on clothing design and body scanning. *Ergonomics* 2017; 60: 1123–1136.

16. Parker C, Gill S and Hayes S. 3D Body Scanning has Suitable Reliability: An Anthropometric Investigation for Garment Construction. In: *Proceedings at 8th international conference and exhibition on 3D body scanning and processing technologies*, Montreal, Canada, 11 October 2017.

17. Špelić I and Petrak S. Complexity of 3D human body scan data modelling. *Tekstilec* 2018; 61: 235–244.

18. Petrak S and Mahnič Naglic M. Dynamic anthropometry – defining protocols for automatic body measurement. *Tekstilec* 2017; 60: 254–262.

19. Lapkovska E and Dāboliņa I. Sizing for a special group of people: best practice of human body scanning, environment, technology. In: *Proceedings of the 12th international scientific and practical conference vol. 1*, 20 June 2019. Rezekne: Rezekne Academy of Technologies.

20. Parker CJ, Gill S, Harwood A, et al. A method for increasing 3D body scanning's precision: gryphon and consecutive scanning. *Ergonomics* 2022; 65(1): 39–59.

21. Rudolf A, Stjepanovič Z and Cupar A. Study regarding the kinematic 3D human-body model intended for simulation of personalized clothes for a sitting posture. *Materials* 2021; 14(18): 5124.

22. Harih G, Kaljun J and Dolšak B. Influence of product interface material stiffness on human tactile perception during a grasping task. *Appl Sci* 2022; 12(17): 8867.

23. Harih G, Kalc M, Vogrin M, et al. Finite element human hand model: validation and ergonomic considerations. *Int J Ind Ergon* 2021; 85(103186). DOI: 10.1016/j.ergon.2021.103186.

24. Magnenat – Thalmann N and Thalmann D. *Handbook of Virtual Humans*. Chichester: John Wiley & Sons Ltd, 2004.

25. Kim S and Park CK. Parametric body model generation for garment drape simulation. *Fibers Polym* 2004; 5: 12–18.

26. Wang CCL. Parameterization and parametric design of mannequins. *Comput Aided Des* 2005; 37(1): 83–98.

27. Magnenat-Thalmann N. *Modeling and simulating bodies and garments*. London: Springer-Verlag, Ltd, 2010.

28. Chu CH, Tsai YT, Wang CCL, et al. Exemplar-based statistical model for semantic parametric design of human body. *Comput Ind* 2010; 61: 541–549.

29. Liu YJ, Zhang DL and Yuen MMF. A survey on CAD methods in 3D garment design. *Comput Ind* 2010; 61: 576–593.

30. Lee KS and Song HK. Automation of 3D average human body shape modeling using rhino and grasshopper algorithm. *Fashion Text* 2021; 8(1): 23–20.

31. Bozic M, Kau CH, Richmond S, et al. Facial morphology of Slovenian and Welsh white populations using 3-dimensional imaging. *Angle Orthod* 2009; 79(4): 640–645.

32. Park TJ, Lee SH and Lee KS. A method for mandibular dental arch superimposition using 3D cone beam CT and orthodontic 3D digital model. *Korean J Orthod* 2012; 42(4): 169–181.

33. PRA, Application of 3D body scanning technology to human measurement for clothing fit. *Int J Digit Content Technol Appl* 2010; 4(7): 58–68.

34. Daanen HAM and Psikuta A. 3D body scanning. In: Nayak R and Padhye R (eds) *The textile institute book series, automation in garment manufacturing*. UK: Woodhead Publishing, Elsevier Ltd., 2018, pp.237–252.

35. Kazhdan M, Bolitho M and Hoppe H. Poisson surface reconstruction. In: *Proceedings of the fourth eurographics symposium on geometry processing (SGP '06)*, Sardinia, Italy, 26 June 2006. Eurographics Association.

36. Kazhdan M and Hoppe H. Screened Poisson surface reconstruction. *ACM Trans Graph* 2013; 32(3): 1–13.

37. Liu Z, Wang L, Tahir M, et al. An improved Poisson surface reconstruction algorithm based on the boundary constraints. *Int J Adv Comput Sci Appl* 2023; 14(1): 225–232.

38. MeshLab webpage. https://www.meshlab.net/ (accessed 2 November 2023).

39. HP SLS scanner. https://support.hp.com/si-en/drivers/selfservice/hp-3d-structured-light-scanner/ (accessed 2 November 2023).

40. 3 D Systems. Sense™ 2 3D scanner, https://s3.amazonaws.com/dl.3dsystems.com/binaries/support/sense-scanner/Sense2_UserGuide_031519.pdf (accessed 2 November 2023).

41. Sperber M. Quadtree and octree. In: Shekhar S, Xiong H and Zhou X (eds) *Encyclopedia of GIS*. Berlin: Springer, 2017.

42. Laser Safety Facts. https://www.lasersafetyfacts.com/laser-classes.html (accessed 2 November 2023).

43. GOM Software. https://mailassets.gom.com/user_upload/software/Whats_new_GOM-Software-2019_EN.pdf (2019, accessed 2 November 2023).

44. Kozar T, Rudolf A, Cupar A, et al. Designing an adaptive 3D body model suitable for people with limited body abilities. *J Textile Sci Eng* 2014; 4: 1–13.

45. Torres-Restrepo AM, Quintero-Monsalve AM, Giraldo-Mira JF, et al. Agreement between cranial and facial classification through clinical observation and anthropometric measurement among Envigado school children. *BMC Oral Health* 2014; 14: 50.

46. Uzomba GC, Obijindu CA and Ezemagu UK. Considering the lip print patterns of Ibo and Hausa ethnic groups of Nigeria: checking the wave of ethnically driven terrorism. *Crime Sci* 2023; 12(1): 4.

47. Leth-Steensen W. Eye socket: the bones that protect your eyes, https://www.allaboutvision.com/eye-care/eye-anatomy/eye-socket/ (2021, accessed 2 November 2023).

48. ISO 5084:1996. Textiles — Determination of thickness of textiles and textile products. 2nd edn. 1996.

49. ISO 3801:1977. Textiles — Woven fabrics — Determination of mass per unit length and mass per unit area. 1st edn. 1977.